The 9th International Supercritical CO_2 Energy Technologies Symposium
March 2–5, 2026, Pittsburg, PA
Paper #027

Effects of Prandtl's Secondary Flows of the Second Kind on sCO_2 Heat Transfer

Christopher M. Bochenek
Undergraduate Student
Department of Aerospace Engineering
Embry-Riddle Aeronautical University

Nicholas C. Lopes
Ph.D. Candidate
Department of Mechanical Engineering
Embry-Riddle Aeronautical University

Mark A. Ricklick
Associate Professor
Department of Aerospace Engineering
Embry-Riddle Aeronautical University

Sandra K.S. Boetcher
Professor
Department of Mechanical Engineering
Embry-Riddle Aeronautical University

ABSTRACT

Prandtl's secondary flows of the second kind appear in turbulent flows within non-circular ducts and are driven by Reynolds stress anisotropy near the corners. Despite significant theoretical, numerical, and experimental efforts to quantify this phenomenon, their influence on supercritical fluid flows have yet to be explored. In the present study, supercritical carbon dioxide (sCO_2) was simulated in a square duct to investigate Prandtl's secondary flows and their effects on local heat transfer behavior. To balance solution accuracy with computational requirements, a Reynolds-Averaged Navier Stokes (RANS) approach was employed over higher-fidelity techniques like large eddy simulation (LES) or direct numerical simulation (DNS). However, most widely adopted RANS turbulence models in the sCO_2 literature employ the Boussinesq eddy viscosity hypothesis, which cannot capture Reynolds stress anisotropy. Thus, a Reynolds stress model (RSM) was selected where each Reynolds stress component is modeled individually. Due to the lack of high-fidelity sCO_2 data in non-circular ducts, The RSM was first tuned and validated against sCO_2 DNS data in a circular duct. The duct had a diameter D = 2 mm and length $L = 30D$, operated with a bulk Reynolds number Re_b = 5400 and pressure P = 8 MPa, and was subjected to a wall heat flux q_w = -30.87 kW m^{-2}. Simulations were then conducted in the square duct under the same conditions. Significant deviations in local quantities were found between the RSM results and additional simulations with the $k-\omega$ shear stress transport (SST), highlighting the need to account for such secondary flow effects.

INTRODUCTION

Prandtl's secondary flows of the second kind are a characteristic feature of turbulent flows in non-circular ducts and are caused by Reynolds stress anisotropy [1, 2]. In non-circular ducts, dominant transverse turbulent fluctuations near the walls generate tangential fluid motion around the corners. A centrifugal body force arises acting towards the corners along the angular bisectors [3]. Consequently, higher momentum fluid from the core is transferred towards the corners and then dispersed along neighboring walls. This manifests as pairs of transverse vortices near the corners that redistribute momentum and energy across the duct's cross-section.

In the present study, and for the first time, Prandtl's secondary flows of the second kind are investigated in a supercritical fluid. Supercritical carbon dioxide (sCO_2) was selected as the working fluid for its applicability to various power generation [4, 5], refrigeration [6], electronic cooling [7], and hypersonic [8] systems. To capture Reynolds stress anisotropy, simulations were conducted using a Reynolds Stress Model (RSM) which balances solution accuracy and practicality. Since the sCO_2 literature lacks high-fidelity DNS studies in non-circular ducts, the RSM was first tuned and validated against local DNS data for sCO_2 in a circular duct. A square duct with hydraulic diameter D = 2 mm and length $L = 30D$ was then simulated to study the desired corner effects. Simulations were conducted without gravity in an attempt to isolate Prandtl's secondary flows from other secondary currents caused by buoyancy. The flow had a bulk Reynolds number Re_b = 5400 and was subjected to a cooling wall heat flux q_w = -30.87 kW m^{-2} at a pressure P = 8 MPa. To highlight the effects of anisotropy, additional simulations were conducted using the $k-\omega$ shear stress transport (SST) turbulence model, a common selection for sCO_2 flows [9, 10, 11, 12]. Local heat transfer and flow data were compared between the two turbulence models.

METHODOLOGY

Operating and Boundary Conditions

The simulations carried out in the circle and square ducts used similar operating and boundary conditions. Both were constructed with a hydraulic diameter of $D = 2$ mm and a streamwise test section length of $L = 30D$. In this test section, a constant cooling heat flux boundary condition was applied; in accordance with other sCO_2 literature and the selected model validation material, the wall heat flux was selected to be $q_w = -30.87$ kW m^{-2}. The operating pressure of the working sCO_2 was set to $P = 8$ MPa with an operating temperature $T = 342.05$ K. A mass flux inlet boundary condition was selected to achieve an inlet bulk Reynolds number $Re_b = \frac{GD}{\mu_b}$ of 5400 with a mass flux $G = 53.8$ kg m^{-2} s^{-1} to match present DNS literature data for model validation. An adiabatic inlet of length $50D$ was placed before the test section to ensure the complete hydrodynamic development of the flow with the mass flux inlet prior to any heat transfer. A pressure outlet was selected for the simulations. A schematic for the duct geometries are provided in Fig. 1. Excess adiabatic domains were considered acceptable for the simulations because of the low computational cost of the selected RANS turbulence models. In order to focus on the effects of Prandtl's Secondary Flows of the Second Kind, a purely forced convection case (i.e. no gravity) was considered for all flows in this study to remove any secondary flow effect due to buoyancy.

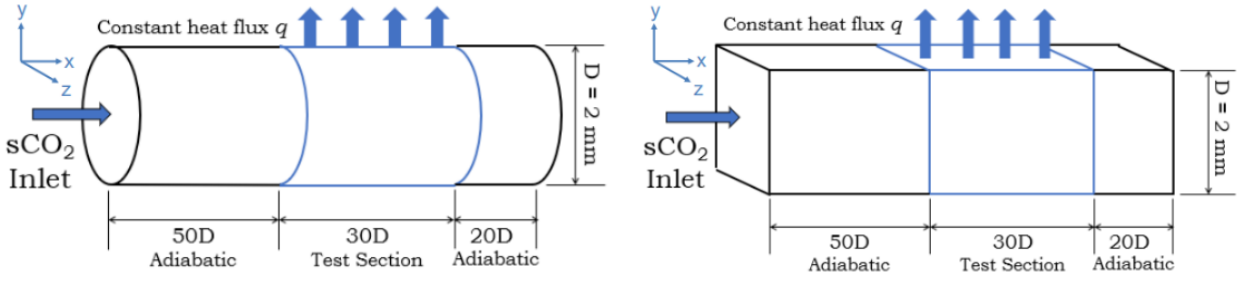

(a) Circular duct geometry

(b) Square duct geometry

Fig. 1 Domains of the circular and square ducts

Meshing and Numerical Procedure

Solving of the Favre-averaged conservation equations and the Reynolds stress tensor using the RSM was completed with the finite-volume method within the ANSYS Fluent software. A $k-\epsilon$ method with linear pressure-strain modeling and enhanced wall treatment was chosen to resolve the entire boundary layer up to the viscous sublayer due to the importance of accurately capturing the local physics near the wall.

For the meshes, both circular and square duct meshes only featured one constraint: the entire boundary layer be resolved up to the wall. The $k-\epsilon$ RSM used enhanced wall treatment, which requires that the first cell height corresponds to a dimensionless wall distance $y^+ < 1$. This dimensionless wall distance value is defined as $y^+ = yu_{\tau.0}/\nu_0$ and is expressed in wall length units. For the present meshes, reported average y^+ values were $y^+ \approx 0.3$.

During the solving process, the heat flux boundary condition was steadily ramped up over iterations. During this ramp-up, the solver used first-order discretization schemes when solving the transport variables for stability. Once the target heat flux was reached, second-order schemes were then used for solution refinement and accuracy. For post-processing, the static enthalpy on any given cross-section was averaged by mass-weighting and an external NIST property table script recovered all thermophysical property data values.

RESULTS

RSM Validation in a Circular Duct

To validate the RSM, DNS literature in sCO_2 was explored. The forced convection results from a cooling study on sCO_2 in a circular microchannel published by Pandey et al. [13] were used for model validation. Their boundary and operating conditions mirror the values in the present study. The circular microchannel was chosen due to the scarcity of DNS literature in square microchannels. To maximize confidence in the results given the available validation, the boundary and operating conditions in the square microchannel were replicated from the circular duct validation runs so as to ensure a similar bulk Reynolds number at the inlet.

The SST and RSM both require parameter fine-tuning to properly match DNS data. The SST was not able to replicate DNS data by solely tuning the turbulent Prandtl number unlike the RSM. For the RSM, the turbulent Prandtl number of the flow was systematically varied until solution agreement with DNS. The various different models discussed in [14] were tested with the RSM. Standard and modified versions of the TWL model, as well as the Kays model, were unable to closely capture the wall temperature. The turbulent Prandtl number that best matched the wall temperature with DNS was a constant $Pr_t = 2$. For all RANS turbulence simulations in the current study, the turbulent Prandtl number was set to $Pr_t = 2$; this includes the square duct simulations.

Bulk temperature, wall temperature, streamwise velocity, and bulk Nusselt number were compared against DNS [13]. The RSM in Fig. 2a features a near exact bulk temperature solution to DNS. Wall temperature data in Fig. 2b follows similar trends with a small dip in the DNS solution, then the values plateau. The bulk Nusselt number RSM solution is able to capture the shape of the DNS curve well as seen in Fig. 2c, with minor variations present consistent with the small deviations in the wall temperature. The RSM additionally shows excellent agreement with the DNS trend in Fig. 2d, suggesting that the model has a strong capability in capturing momentum transport.

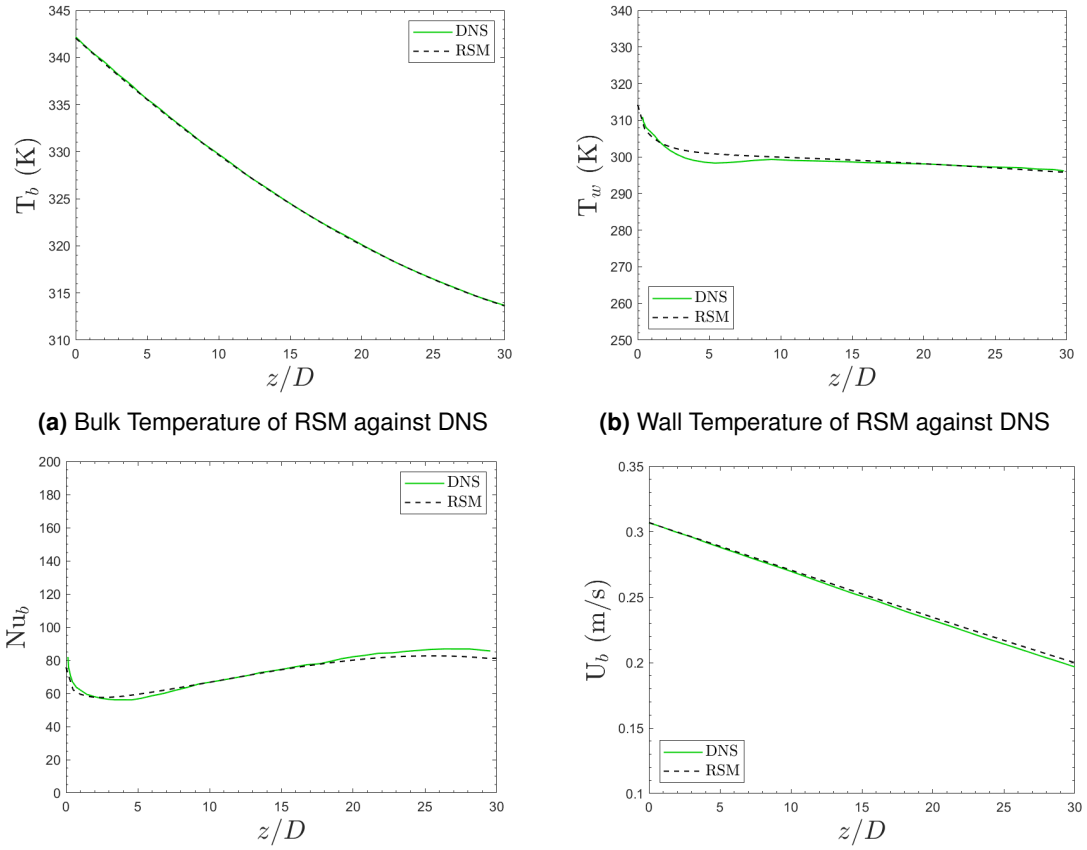

(a) Bulk Temperature of RSM against DNS

(b) Wall Temperature of RSM against DNS

(c) Bulk Nusselt number of RSM against DNS

(d) Bulk Velocity of RSM against DNS

Fig. 2 RSM Validation of data along Test Section against DNS

RSM Square Results

To compare the RSM against existing isotropic RANS models with Prandtl's Secondary Flows of the Second Kind present in the duct geometry, the $k-\omega$ SST model was used as a baseline, both with and without its corner-correction option, to approximate the flow behavior within the corners of the square duct. The $k-\omega$ SST model was selected for its widespread adoption as a default RANS approach in both research and industry.

SST and RSM heat transfer data were recorded in the square duct to capture the differences in the RANS models. The greatest deviance in solution data between the SST and RSM was within the bulk temperature data as seen in Fig. 3a. Bulk temperature data varied with a RMSE of 5.23 K between the RSM and SST. Wall temperature and bulk Nusselt number of the SST options follow closely with the RSM, with the corner-correction setting providing a higher deviation from the RSM as seen in Figs. 3b, 3c. SST also features a large deviation from the RSM when solving for bulk velocity, with a RMSE of 0.022 m s^{-1} in Fig. 3d. This elevated RMSE suggests inconsistencies in the solution of the momentum transport equations when compared with the RSM data.

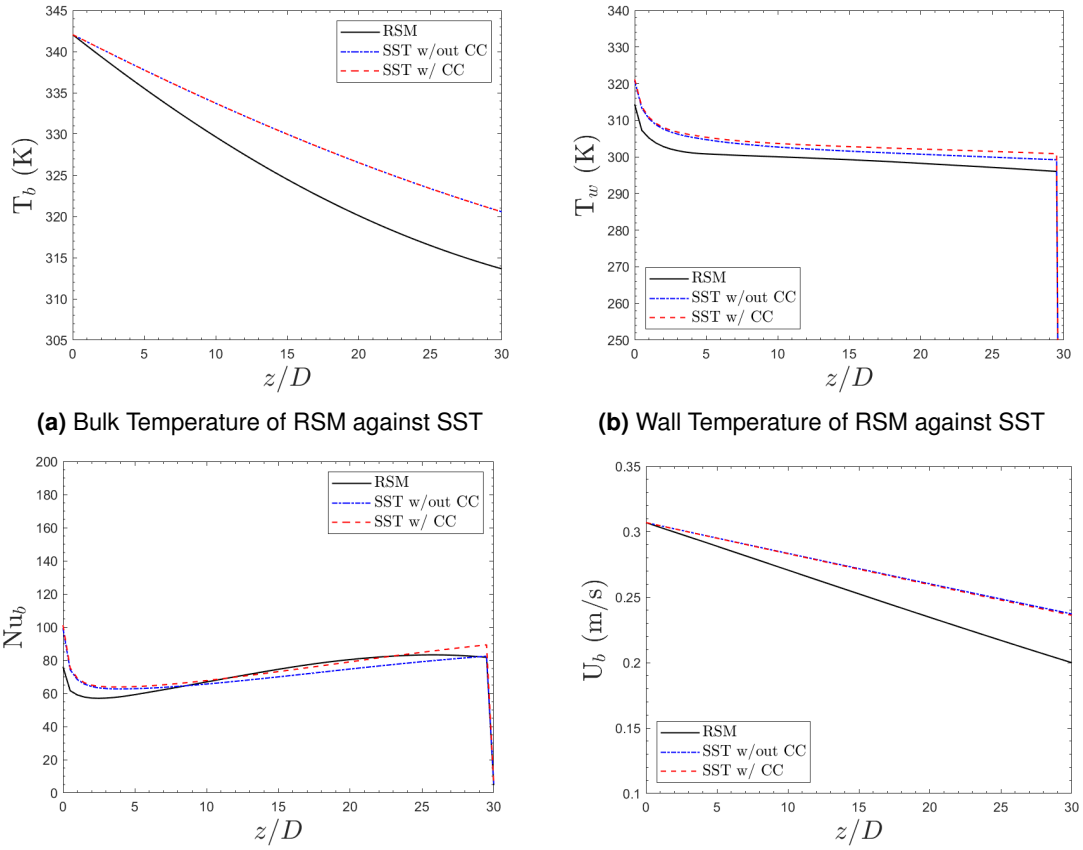

(a) Bulk Temperature of RSM against SST

(b) Wall Temperature of RSM against SST

(c) Bulk Nusselt number of RSM against SST

(d) Bulk Velocity of RSM against SST

Fig. 3 RSM Validation of data along Test Section against RANS

CONCLUSIONS

Within the sCO_2 literature, the effects of Prandtl's Secondary Flows of the Second Kind are not extensively investigated. While LES and DNS simulations are able to capture the anisotropy of the flow, they are computationally expensive and limited to lower Reynolds number flow domains. RANS models are cheap, but many assume isotropy of the flow and are not able to catch the physics due to these secondary flows. The proposed RSM is a good compromise between lower-order RANS modeling and higher-accuracy methods.

The RSM was able to strongly replicate DNS results in a circular duct with turbulent Prandtl number tuning. In order to ensure the validation is as meaningful as possible, the RSM was tested in a square duct with the same flow conditions and hydraulic diameter. Gravity and buoyancy effects were not included as to isolate Prandtl's Secondary Flows of the Second Kind from secondary flows caused by buoyancy.

In the square duct, the RSM was ran with $k-\omega$ SST, both with and without the available corner-correction setting to highlight the differences between the RSM and SST and its shortcomings. The largest differences were between bulk temperature and velocity, where the RSM reported lower temperature values. This is primarily due to the RSM being able to record the swirling of the flow in corners, which convects warmer fluid towards the walls and leads to better cooling. Secondary flow velocity magnitude was between 1-2% of the streamwise flow velocity.

REFERENCES

[1] N. V. Nikitin, N. V. Popelenskaya, and A. Stroh. Prandtl's secondary flows of the second kind. problems of description, prediction, and simulation. *Fluid Dynamics*, 56(4):513–538, June 2021. ISSN 1573-8507. doi:10.1134/s0015462821040091.

[2] Khalid A. M. Moinuddin, P. N. Joubert, and M. S. Chong. Experimental investigation of turbulence-driven secondary motion over a streamwise external corner. *Journal of Fluid Mechanics*, 511:1–23, July 2004. ISSN 1469-7645. doi:10.1017/s0022112004008742.

[3] S Ahmed and E Brundrett. Turbulent flow in non-circular ducts. part 1. *International Journal of Heat and Mass Transfer*, 14(3):365–375, March 1971. ISSN 0017-9310. doi:10.1016/0017-9310(71)90156-6.

[4] Yuhui Xiao, Yuan Zhou, Yuan Yuan, Yanping Huang, and Gengyuan Tian. Research advances in the application of the supercritical co2 brayton cycle to reactor systems: A review. *Energies*, 16(21):7367, October 2023. ISSN 1996-1073. doi:10.3390/en16217367.

[5] Jia-Qi Guo, Ming-Jia Li, Ya-Ling He, Tao Jiang, Teng Ma, Jin-Liang Xu, and Feng Cao. A systematic review of supercritical carbon dioxide(s-CO2) power cycle for energy industries: Technologies, key issues, and potential prospects. *Energy Conversion and Management*, 258:115437, apr 2022. doi:10.1016/j.enconman.2022.115437.

[6] Orelien T. Boupda, Hyacinthe D. Tessemo, Isidore B. Nkounda Fongang, Francklin G. Nyami, Frederic Lontsi, and Thomas Djiako. A review on technologies for the use of co2 as a working fluid in refrigeration and power cycles. *Energy and Power Engineering*, 16(06):217–256, 2024. ISSN 1947-3818. doi:10.4236/epe.2024.166011.

[7] Sushant Kumar Sharma, Ajay Kumar Yadav, and Mohd.Kaleem Khan. Electronic chip cooling using supercritical carbon dioxide in microchannels. *Applied Thermal Engineering*, 280: 128436, December 2025. ISSN 1359-4311. doi:10.1016/j.applthermaleng.2025.128436.

[8] Xinrui Zhang, Wenjie Guo, Guangjun Gao, Wenxiong Xi, Jian Liu, and Bengt Sunden. Numerical investigations of flow and heat transfer characteristics of a regenerative cooling channel using supercritical co2 with different cross-section shapes. *International Journal of Thermal Sciences*, 215:109965, September 2025. ISSN 1290-0729. doi:10.1016/j.ijthermalsci.2025.109965.

[9] Nicholas C. Lopes, Yang Chao, Mark A. Ricklick, and Sandra K.S. Boetcher. Influence of thermal boundary conditions on local supercritical co2 cooling heat transfer: A case study. *International Journal of Heat and Fluid Flow*, 106:109310, April 2024. ISSN 0142-727X. doi:10.1016/j.ijheatfluidflow.2024.109310.

[10] Nicholas C. Lopes, Mark A. Ricklick, Sandra Boetcher, and Yang Chao. Impact of inlet conditions on local sco2 cooling heat exchanger performance. In *AIAA SCITECH 2025 Forum*. American Institute of Aeronautics and Astronautics, January 2025. doi:10.2514/6.2025-2846.

[11] Yang Chao, Nicholas C. Lopes, Mark A. Ricklick, and Sandra K. S. Boetcher. Impact of adiabatic entrance length on numerical simulations of supercritical co2 heat transfer in horizontal circular tubes. *Numerical Heat Transfer, Part A: Applications*, pages 1–27, December 2023. ISSN 1521-0634. doi:10.1080/10407782.2023.2287534.

[12] Yang Chao, Nicholas C. Lopes, Mark A. Ricklick, and Sandra K. S. Boetcher. Effect of the heat transfer coefficient reference temperatures on validating numerical models of supercritical CO2. *Journal of Verification, Validation and Uncertainty Quantification*, 6(4):041001, 2021. doi:10.1115/1.4051637.

[13] Sandeep Pandey, Xu Chu, and Eckart Laurien. Investigation of in-tube cooling of carbon dioxide at supercritical pressure by means of direct numerical simulation. *International Journal of Heat and Mass Transfer*, 114:944–957, November 2017. ISSN 0017-9310. doi:10.1016/j.ijheatmasstransfer.2017.06.089.

[14] Binhui Yu, Yanjuan Wang, Qibin Liu, Weijie Shi, and Jinliang Xu. Effects of turbulent prandtl number on supercritical carbon dioxide turbulent flow with high heat flux in vertical round tube. *Applied Thermal Engineering*, 249:123310, 2024. ISSN 1359-4311. doi:https://doi.org/10.1016/j.applthermaleng.2024.123310.